Polym. Bull. (2017) 74:465–482
DOI 10.1007/s00289-016-1724-1

ORIGINAL PAPER

Analysis of dynamic oscillatory rheological properties of PP/EVA/organo-modified LDH ternary hybrids based on generalized Newtonian fluid and generalized linear viscoelastic approaches

Masoud Razavi Aghjeh[1] · Elham Mardani[2] · Faezeh Rafiee[2] · Maryam Otadi[2] · Hossein Ali Khonakdar[3,4] · Seyed Hassan Jafari[4] · Uta Reuter[4]

Received: 12 April 2016 / Revised: 7 June 2016 / Accepted: 9 June 2016 /
Published online: 20 June 2016

Abstract A comprehensive investigation was performed on single-step melt processed polypropylene (PP)/(ethylene vinyl acetate copolymer (EVA)/organo-modified layered double hydroxide (LDH) counterpart ternary hybrids to explore the effect of LDH loading on small-amplitude oscillatory shear (SAOS) rheological properties and to correlate the properties with microstructure. The rheological results were analyzed in detail from qualitative and quantitative perspectives. Using qualitative interoperation of storage modulus and complex viscosity alteration against LDH loading, and also quantitative analysis by viscosity models based on both the generalized Newtonian fluid (GNF) and generalized linear viscoelastic (GLVE) approaches, detailed predictions were carried out on the microstructure of samples and also partitioning of the organo-modified LDH particles and their intercalation and exfoliation extent within hybrids. By comparing the elasticity and relaxation spectrum of PP-rich/LDH with those of EVA-rich/LDH hybrids, it was predicted that organo-modified LDH platelets, in the case of PP-rich samples, have been located at the interface or within the EVA dispersed particles, while in the case of EVA-rich samples, they mainly localized within the matrix. In addition, the crossover frequency and slope of G' and G'' curve at terminal region were correlated with the extent of intercalated and exfoliated structures of filler. The validity of these predictions on microstructure of the developed hybrids was confirmed visually using transmission electron microscope (TEM) micrographs.

✉ Hossein Ali Khonakdar
hakhonakdar@gmail.com

[1] School of Chemical Engineering, College of Engineering, University of Tehran, Tehran, Iran

[2] Department of Chemical Engineering, Faculty of Engineering, Central Tehran Branch, Islamic Azad University, P.O. Box 19585-466, Tehran, Iran

[3] Department of Polymer Engineering, Faculty of Engineering, South Tehran Branch, Islamic Azad University, P.O. Box 19585-466, Tehran, Iran

[4] Leibniz Institute of Polymer Research, 01067 Dresden, Germany

Keywords Organo-modified layered double hydroxide (LDH) · Morphology · Rheology

Introduction

There are various kinds of standard flows [1–3] to study the rheological properties of non-Newtonian fluids which all are similar in basics. In these methods, a material is subjected to defined stress or strain, and then, its response to the imposed stress or strain is measured. All the standard flows can be categorized in two sets of flows, i.e., shear and elongation [4]. In addition, in all kinds of these experiments, various types of material functions are defined to make relation between stress and strain data pairs. In the simple shear flow (SSF), where velocity profile ($\underline{\upsilon}$) is defined as Eq. 1, depending on shear-rate function ($\dot{\varsigma}(t)$), different types of flows, and accordingly different types of material functions can be defined. Among the SSFs, small-amplitude oscillatory shear (SAOS) flow, in which the shear-rate function is equal to $\dot{\gamma}\cos\omega t$ ($\dot{\gamma}$ amplitude of shear-rate, ω frequency of experiment) [4], the two material functions of storage (G'), and loss modulus (G''), are defined to correlate the imposed shear rate to recorded stress. This type of flow as a result of its ability to preserve microstructure of material and to reveal considerable information about microstructure of polymeric filled systems has been attracted great deal of attentions of rheologists.

$$\underline{\underline{\upsilon}} = \begin{pmatrix} \dot{\varsigma}(t)x_2 \\ 0 \\ 0 \end{pmatrix}_{123} \tag{1}$$

Polypropylene (PP) and ethylene vinyl acetate copolymer (EVA) are two subcategories of polyolefins with exceptional properties, including excellent chemical and moisture resistance, good processability, low density, and also relatively low price level [5–7]. These features turn them as the most versatile commodity polymers. However, both of these polymers have some drawbacks, such as low impact strength for PP and low modulus for EVA [8]. Their complementary properties, i.e., low impact strength and high modulus of PP and low modulus and high impact strength of EVA, along with good compatibility between these materials in melt state, make them as a suitable pair to produce polyolefinic materials with adjustable balance of properties. The other main drawback of polyolefins is their low thermal resistance, particularly when the material is exposed to high temperature and voltages in applications, such as wire and cable coatings [9]. Among the various additives which are added to improve thermal and flame properties of polyolefins, recently, layered double hydroxides (LDHs) have been attracted growing interest. The LDHs are a class of anionic or hydrotalcite-like clays represented by the general formula $[M^{II}_{1-x}M^{III}_{x}(OH)_2]^{x+}.[(A^{n-})^{x/n}.mH_2O]$, where M^{II} and M^{III} are divalent and trivalent metal cations, respectively, and A^- is the interlayer anion [10]. These materials because of their typical metal-hydroxide-like chemistry and conventional clay-like layered crystalline structure, through

endothermic decomposition and char formation donate higher thermal and flame properties to the polymeric matrix [10]. In addition to thermal properties, these materials as a result of their high aspect ratio, similar to nanoclays, can improve mechanical properties of sample to a considerable level [11].

Although there are some reports on rheological and morphological properties of PP/LDH and EVA/LDH individual hybrids. However, to the best of our knowledge, there are no comprehensive studies on rheological and morphological properties of PP/EVA blends containing different loadings of organo-modified LDH. The main objective of present work is to explore the effect of organo-modified LDH loading on small-amplitude oscillatory shear (SAOS) rheological properties of PP-rich and EVA-rich counterpart blends and to correlate the rheological properties with microstructure. The other objective is to predict microstructure of the developed hybrids, i.e., blend morphology as well as partitioning of organo-modified LDH and their intercalation and exfoliation states within blend components based on the detailed qualitative and quantitative analyses of rheological data using generalized Newtonian fluid (GNF) and generalized linear viscoelastic (GLVE) approaches.

Experimental part

Materials

PP (Moplen HP501H; density = 0.9 g/cm^3, MFI at 230 °C and 2.16 kg = 2.1 g/10 min) from Basell and EVA (Escorene Ultra UL00218CC3; density = 0.94 g/cm^3, MFI at 190 °C and 2.1 6 kg = 1.7 g/10 min, vinyl acetate content = 18 wt%,) from Exxon Mobile Chemical Company were used as received. Magnesium nitrate and aluminum nitrate and sodium dodecyl benzene sulfonate (SDBS) used for the synthesis of organo-modified Mg–Al-layered double hydroxide (LDH) by one-step route were obtained from Merck. Prior to melt blending, all the materials were dried for 24 h at 60 °C in a vacuum oven.

Synthesis of organo-modified LDH

The organo-modified LDH was synthesized in one-step process according to the following procedure: briefly, an NaOH solution was added dropwise to an aqueous sodium dodecylbenzene sulfonate (SDBS) solution in a 250-mL three round-bottomed flask, and then, a solution of magnesium nitrate and aluminum nitrate (with Mg^{2+}:Al^{3+} equal to 2:1 and a total metal ion concentration of 0.3 M) was added dropwise to the flask. During the reaction, solution was stirred for 30 min at 50 °C, and the pH value was kept at 10.0 by adjusting with 1-mol/L NaOH. Then, the temperature was increased to 70 °C and allowed to age for 24 h. Upon cooling, final white products was collected by filtration and washed thoroughly with distilled water to a neutral pH and dried in oven at 75 °C.

Processing

16 samples, including pure PP and EVA, PP and EVA containing 1, 3 and 7 wt% of LDH coded as P1, P3, P7, E1, E3, and E7, 75/25 and 25/75 PP/EVA blends and their corresponding LDH loaded hybrids with 1, 3 and 7 wt% of LDH coded as 75/25/1, 75/25/3, 75/25/7, 25/75/1, 25/75/3, and 25/75/7, were prepared in a twin-screw micro compounder MC15 (Xplore, The Netherlands) at the temperature of 190 °C and under screw speed of 200 rpm and processing time of 5 min. Then, to freeze the morphology of the compounded materials, they were submerged in a cold water bath and dried in a vacuum oven at 60 °C for 24 h.

Characterizations

Rheological measurements

Dynamic rheometry in the melt state was carried out using stress controlled rheometer (Anton Paar MCR301) equipped with parallel plate geometry (diameter = 25 mm, gap = 1 mm). The samples were prepared as discs of 25-mm diameter and 2-mm thickness by compression molding. All measurements were done in a dry nitrogen atmosphere to suppress oxidative degradation. To achieve thermal equilibrium and structural relaxations, a waiting time after loading was applied before the measurements. Dynamic strain sweeps showed that rheological measurements performed at strain of 5 %, safely fall within linear viscoelastic limit. Then, dynamic frequency sweeps were performed in the frequency range of 0.01–600 rad/s at fixed temperature of 200 °C.

Morphological studies

A transmission electron microscope (TEM LIBRA 120, 120 kV, Carl Zeiss, Germany) was used to investigate the dispersion quality of the LDH particles within the matrix, partitioning of its platelets between blend components, and the microstructure of the samples. The samples were cryo-microtomed at −120 °C by means of an ultramicrotome EM UC6/FC6, Leica, Austria.

Results and discussion

Rheology

Storage modulus and complex viscosity

Storage modulus (G') and loss modulus (G'') are the two material functions that conclude directly from SAOS experiment. These material functions are related to complex viscosity magnitude ($|\eta^*|$) using the following relation:

$$|\eta^*| = \frac{\sqrt{G'^2 + G''^2}}{\omega} \ (\omega: \text{ amplitude of experiment}). \tag{2}$$

Since G' is more sensitive to morphological and microstructural changes [12] and also magnitude of η^* is interpretable as steady shear viscosity (η) in terms of Cox–Merz rule [13] (Eq. 3), only these two material functions (G' and η^*), are considered in interpretation of results in the following paragraphs.

$$\eta(\dot{\gamma}) = |\eta^*|_{\dot{\gamma}=\omega} \ (\dot{\gamma}: \text{ shear-rate at steady shear experiment}) \tag{3}$$

Figure 1 represents the mentioned material functions for the pure PP and EVA and their blends. Both of PP and EVA show complete power-law behavior at low and intermediate frequencies and also tendency to plateau at higher frequencies in their G' curves. Moreover, in low and intermediate range of frequencies, the elasticity/viscosity of EVA is more than that of PP. While, as frequency increases, the inverse behavior is detectable. This behavior stems from more shear-thinning nature of EVA as compared to PP. In addition, the breadth of non-Newtonian region in the case of PP is more than that of EVA. These can be attributed to wider molecular weight distribution and/or copolymeric architecture of EVA chains [14]. Blends of PP and EVA because of their biphasic microstructure and relaxation phenomena associated with interface do not show the power low and Newtonian behavior of pure polymers in terminal regions of their G' and $|\eta^*|$ curves, respectively. Furthermore, it is seen that at low frequencies elasticity and viscosity curves of both 75/25 and 25/75 blends situate above their pure components, even higher than those of EVA. Positive deviation from linear mixtures rule in G' and $|\eta^*|$ at low frequencies has been observed in the phase-separated polymeric blends and attributed to interfacial compatibility and its associated relaxation process [15]. In spite of higher viscosity/elasticity of EVA than that of PP, when frequency increases elasticity and viscosity values of 75/25 prevail over its counterpart sample, i.e., 25/75. The inverse behavior at lower and higher frequencies results from higher shear-thinning nature of 25/75 which itself originates from higher shear-thinning nature of its matrix and/or weaker interfacial compatibility between phases of this blend as compared to that of 25/75.

Effect of adding different loadings of LDH into PP and EVA on their G' and $|\eta^*|$ has been represented in Fig. 2; addition of LDH into PP and EVA leads to increment of G' at low frequencies and deviation from terminal behavior, especially at concentrations higher than 1 wt%. In general, complex viscosity of samples increases by enhancement of LDH content and also deviates from Newtonian behavior at low frequencies. In the case of 1 wt% of LDH viscosity enhancement is detectable at the whole range of frequency, on the other hand for higher concentrations, the presence of LDH platelets results in reduction of viscosity/elasticity at higher and intermediate frequencies. Enhancement of elasticity/viscosity at lower frequencies is due to the retardation in relaxation of polymeric chains as a result of restriction imposed by filler particles. In addition, the reduction of elasticity/viscosity at higher frequencies originates from orientation of platelets in direction of flow, disentanglement, and shear-thinning effect imposed by these

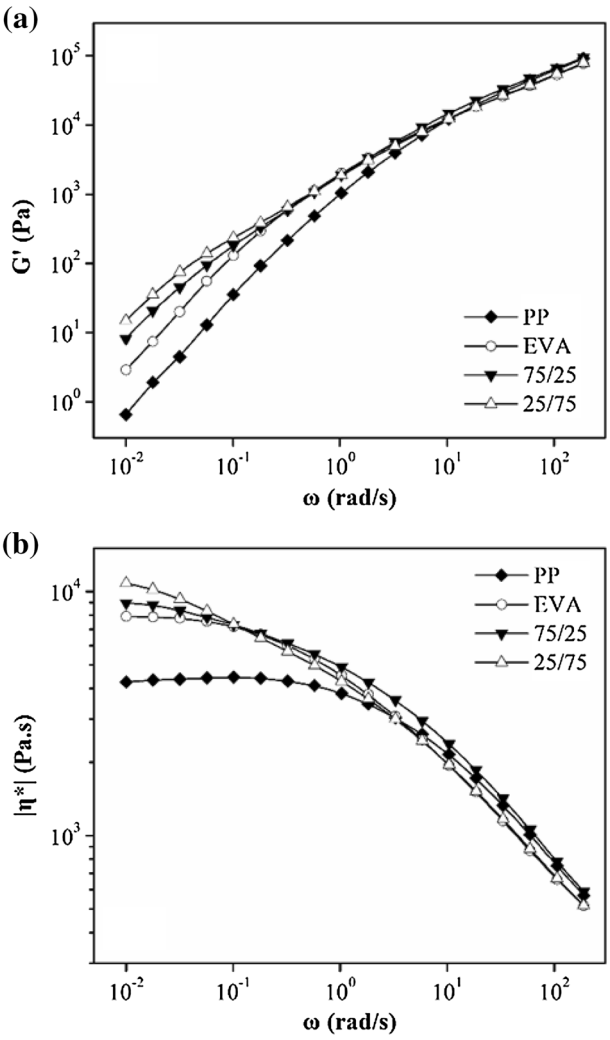

Fig. 1 **a** Storage modulus and **b** complex viscosity of PP, EVA, and their blends as a function of angular frequency

particles [16]. The storage modulus enhancement at the least frequency ($\omega = 0.01$ rad/s) in the case of PP and EVA and at 7 wt% of LDH are equal to 35 and 16 Pa, respectively; however, extent of change in trend of G' curves in these two systems (PP/LDH and EVA/LDH hybrids) is almost indistinguishable. On the other hand, comparing their complex viscosity curves indicates that effect of LDH addition on deviation from Newtonian behavior and enhancement of zero-shear viscosity at low frequencies and also on imposing shear-thinning behavior at intermediate and high frequencies is higher in EVA/LDH system as compared to PP/LDH hybrid. This implies the higher potential of EVA chains to penetrate into

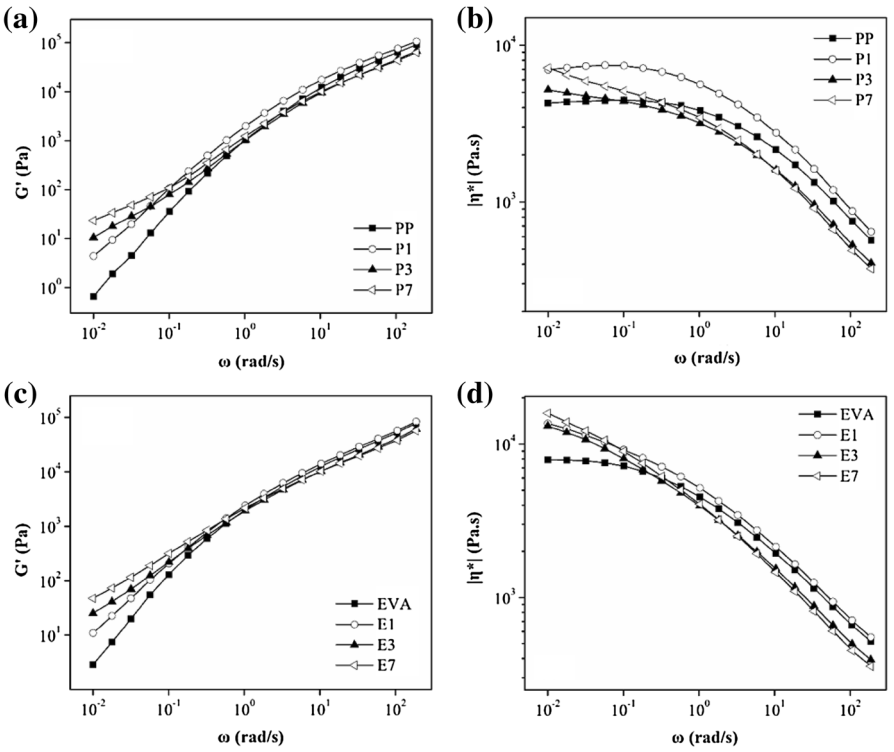

Fig. 2 **a**, **c** Storage modulus and **b**, **d** complex viscosity magnitude of PP/LDH and EVA/LDH hybrids at varying wt% of LDH as a function of angular frequency

galleries of LDH particles. Since polarity of EVA chains is more than that of PP [17] molecules, previous conclusion, i.e., higher tendency of LDH to EVA and vice versa, is not far from the expectation.

Effect of LDH loading on G' and $|\eta^*|$ of 75/25 and 25/75 counterpart blends has been demonstrated in Fig. 3. A close look at G' and $|\eta^*|$ of 75/25/LDH and 25/75/LDH systems shows that for all concentrations of LDH except 1 wt%, the more filler content, the more increase in G' and $|\eta^*|$ of samples at low range of frequencies. It seems that at 1 wt% of LDH, filler particles only act as a conventional filler having weak interaction with matrix, and hence, they increase G' and $|\eta^*|$ in the whole range of frequency by maintaining its trends similar to the unfilled polymers. However, it should be noted that the previous sentence is more accurate in the case of 75/25/1 rather than 25/75/1, especially in $|\eta^*|$ curves, in which for 75/25/1, the Newtonian region has been preserved, while for the 25/75/1, this region has been vanished. This could be other reason that indicates more tendency of LDH toward EVA as compared to its tendency to PP. In our previous paper, it was demonstrated that SAOS experiment can be implemented as a strong tool to determine clay location in PLA/EVA/clay nanocomposites [12]. Similarly, here, some speculations can be made on partitioning of LDH particles within the samples. As it was seen

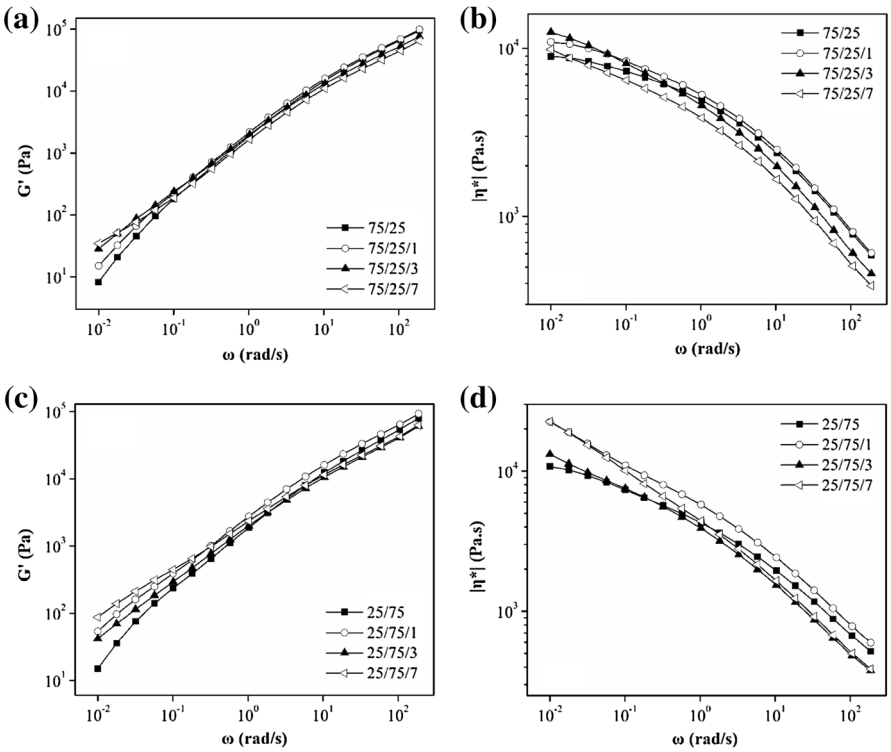

Fig. 3 **a**, **c** Storage modulus and **b**, **d** complex viscosity of 75/25/LDH and 25/75/LDH hybrids at varying LDH loadings as a function of angular frequency

previously, addition of LDH into PP and EVA has almost similar effect on changing of trend of G' curve in both systems, while in the G' curves of Fig. 3a, c, it is seen that storage modulus enhancement at terminal region for the PP-rich ternary hybrids is less than that for EVA-rich ternary hybrids. The observed more elasticity of EVA-rich ternary hybrids than that of PP-rich ternary hybrids may have two reasons; localization of LDH particles in the interface of blend and/or good exfoliation of filler platelets within the matrix. Because of one-step feeding policy and also greater affinity of LDH to EVA than PP, it seems that the first hypothesis has low probability. In addition, since the shear-rate during processing of EVA/LDH samples was the same as its value during processing of 25/75/LDH series of samples and the thermodynamic affinity of LDH to matrix of both samples (in both cases, EVA is matrix) is equal, and also viscosity of 25/75/LDH samples during processing (higher shear rates) is almost equal to that of EVA/LDH samples, the greater exfoliation of LDH platelets in 25/75 in comparison with its exfoliation state in EVA seems impossible. Therefore, it seems in 25/75/LDH samples, LDH particles mainly localize within the EVA matrix and to a great possibility with equal state of exfoliation of corresponding EVA/LDH hybrids. A question may arise that what phenomenon can result in higher G' enhancement in 25/75/LDH samples when

compared to 75/25/LDH hybrids? Bringing up this question in a vice versa manner, i.e., what phenomenon can result in lower G' enhancement in 75/25/LDH samples when compared to 25/75/LDH hybrids? gives this hint to scrutinize the reason in LDH partitioning between phases of 75/25/LDH samples. Again, by considering the similar effect of LDH in G' curves of pure PP and EVA (Fig. 2a, c), greater affinity of LDH to EVA and less increment of G' in 75/25/LDH samples, it seems that LDH particles do not localize mainly within the matrix, so they should be localized at the interface or within dispersed phase. However, since a complete localization at interface results in considerable elasticity enhancement [12], they may have been localized mainly within the EVA dispersed particles. Irrespective of intercalation and exfoliation state of LDH platelets, when filler particles are localized in dispersed phase, they impose less elasticity to the system as compared to the situation, in which the same content of filler particles is situated within the matrix phase [18]. Therefore, in these series of samples (75/25/LDH) with a great possibility, the LDH particles have been mainly localized within the dispersed EVA phase.

The qualitative analysis of two material functions (G' and η^*) was carried out in detail at the above paragraphs. In the following two sections by modeling of rheological data using two different approaches in defining constitutive equations: i) excluding memory effects using generalized Newtonian fluid (GNF) model and ii), including memory effects using generalized linear viscoelastic (GLVE) model, more lights will be shed on microstructural and rheological properties of the hybrid systems in a quantitative manner.

GNF model approach

This method is based on the simple proportionalities between the stress tensor ($\underline{\underline{\tau}}(t)$) and the instantaneous rate of strain tensor ($\underline{\underline{\dot{\gamma}}}(t)$), i.e. $\underline{\underline{\tau}}(t) = -\eta(\dot{\gamma})\underline{\underline{\dot{\gamma}}}(t)$ [19]. Here, among the various models to describe viscosity ($\eta(\dot{\gamma})$), Carreau–Yasuda model [20] is the model that contains more structural parameters and also gives best fit to experimental data of viscosity versus shear rate. Using the Cox-Merz rule (Eq. 2) and also setting infinite viscosity (η_∞) equal to zero, the model is converted to:

$$|\eta^*(\omega)| = \eta_0(1 + (\dot{\gamma}\lambda)^a)^{\frac{n-1}{a}} \tag{4}$$

where η_0 is zero-shear-rate viscosity, a is an exponent representing the sharpness of transition between zero-shear-rate plateau and the power-law like region, λ is relaxation time and attributes to critical shear-rate that accounts for the onset of shear-thinning region, and n relates to the slope of power-law like region. By fitting experimental data of $|\eta^*|$-ω into Eq. 4, the parameters of Carreau–Yasuda viscosity model were calculated and the results are presented in Table 1.

In general, it is observed that adding LDH into different media results in increment of η_0 and reduction of a and n exponents. A closer look at data of Table 1 reveals that effect of LDH on increasing η_0 is more intensive when the media is EVA and EVA-rich, i.e., 25/75 series of samples, as compared to situation, in which filler particles have been added into PP or PP-rich samples. As mentioned

Table 1 Calculated parameters from the Carreau–Yasuda viscosity model and quantitative analysis of G' and G'' curves

Sample	η_0 (Pa.s)	a	λ (s)	n	G' slope	G'' slope	Crossover (rad/s)
PP	4429	0.96	0.30	0.49	1.87	1.03	43.7
P1	7413	0.87	0.46	0.46	1.31	1.05	27.8
P3	5102	0.55	0.32	0.41	0.93	0.92	36.0
P7	8356	0.33	0.07	0.14	0.63	0.84	26.2
EVA	8241	0.76	1.75	0.52	1.63	0.99	46.4
E1	19,250	0.34	1.47	0.40	1.27	0.87	40.0
E3	23,083	0.33	6.40	0.44	0.84	0.84	32.7
E7	29,684	0.35	13.74	0.43	0.76	0.77	20.5
75/25	10,492	0.38	0.14	0.27	1.60	0.96	33.8
75/25/1	14,495	0.31	0.07	0.16	1.32	0.94	30.3
75/25/3	23,964	0.22	0.03	0.00	0.96	0.86	23.7
75/25/7	15,272	0.25	0.05	0.05	0.69	0.82	23.3
25/75	20,518	0.22	0.04	0.12	1.49	0.88	45.0
25/75/1	129,250	0.14	0.01	0.00	1.02	0.69	31.6
25/75/3	167,500	0.13	0.01	0.00	0.90	0.73	26.7
25/75/7	729,360	0.10	0.02	0.00	0.80	0.67	18.9

previously, this is due to the higher thermodynamically tendency of LDH to EVA and also difference in the partitioning of LDH platelets in two series of samples. Reduction in value of a exponent by addition of LDH implies that the presence of filler platelets results in widening of curvature of transient region between zero-shear-rate plateau and power-law like region. In the other words, the presence of LDH fillers results in increment of the range of transition region spanning between Newtonian section and power-law type region of $|\eta^*|$-ω plot. In addition, the observed descending trend in n exponent with respect to addition of filler is due to increment in shear-thinning behavior. Moreover, there is not regular trend in alteration of λ values with LDH loading. It can be concluded that although, Eq. 3 is a more developed viscosity model for generalized Newtonian fluids, however, as it was observed, it cannot reveal more information about microstructural aspects of samples, especially when it comes to calculation of relaxation times, the model gives only a rough single value. Meaninglessness trend in values of λ can be due to this fact that in GNF approach, memory effects, i.e., elastic contribution to relaxation phenomenon, have been excluded. Therefore, in the next section using generalized linear viscoelastic model, the relaxation behavior will be discussed accurately.

GLVE model approach

In this method, in addition to contribution of instantaneous shear-rate, the effect of history of deformation (memory) on stress has been included [21]. To put in another way, in the range of small strains (linear region), it is assumed that the deformation

and stress tensors in a viscoelastic material can be described based on Boltzmann superposition principle [22]:

$$\underline{\underline{\tau}}(t) = -\int_{-\infty}^{t} G(t-t')\underline{\underline{\dot{\gamma}}}(t\prime)dt\prime \tag{5}$$

where $\underline{\underline{\tau}}$ is the stress tensor, $\underline{\underline{\dot{\gamma}}}$ is tensor of deformation rate and G describes material response to flow. One of the applications of GLVE constitutive model is obtaining the discrete relaxation time spectrum [4]. Although, in the data obtained from SAOS experiment, relaxation behavior of polymeric system can be traced using different methods, including G'-ω, tanδ-ω, and Cole–Cole plot (relationship between real (η') and imaginary (η'') parts of complex viscosity [23]); however, relaxation time spectrum can reflect all the relaxation processes in a clearer manner. In addition, some of relaxation processes which are unobservable by other methods can be distinguished by means of relaxation spectrum. By substituting stress and deformation tensors of SAOS into Eq. 5 and describing modulus (G) based on the generalized Maxwell model constituting of N units (Eq. 6),

$$G(t-t') = \sum_{i=1}^{N} H_i \exp[-(t-t')/\lambda_i] \tag{6}$$

where H_i is elastic modulus corresponding to relaxation time of λ_i, the material functions in SAOS measurements can be calculated as follows (Eqs. 7 and 8):

$$G'(\omega_j) = \sum_{i=1}^{N} H_i \frac{(\omega_j\lambda_i)^2}{1+(\omega_j\lambda_i)^2} \tag{7}$$

$$G''(\omega_j) = \sum_{i=1}^{N} H_i \frac{\omega_j\lambda_i}{1+(\omega_j\lambda_i)^2}. \tag{8}$$

Here, j is the number of collected (G', G'', ω) sets of data. By fitting Eqs. 7 and 8 into the recorded data (G', G'' vs ω) and setting N equal to 50, and using edge preserving regularization method described in detail by Roths et al. [24], the discrete relaxation times of samples were calculated. The accuracy of obtained relaxation times depends on quality of fitting of experimental storage and loss moduli with calculated values from Eqs. 7 and 8. In the case of EVA, typical results of calculated G' and G'' along with their experimental counterparts have been shown in Fig. 4. It is clearly seen that there is a good correlation between calculated and experimental values at intermediate and low frequencies. Since relaxation of blends and, especially, filled systems takes place at longer times, correlation between experimental and calculated values in lower and intermediate frequencies, i.e., higher and intermediate relaxation times, owns a great importance in comparison with correlation of their values at higher frequencies (lower relaxation times).

Figure 5 shows the weighted relaxation time spectrum ($\lambda H(\lambda)$ vs λ) for the neat polymers and their blends. In the relaxation spectrum of EVA and PP, there are one broad peak and two narrow peaks, respectively. Theses peaks which all relate to

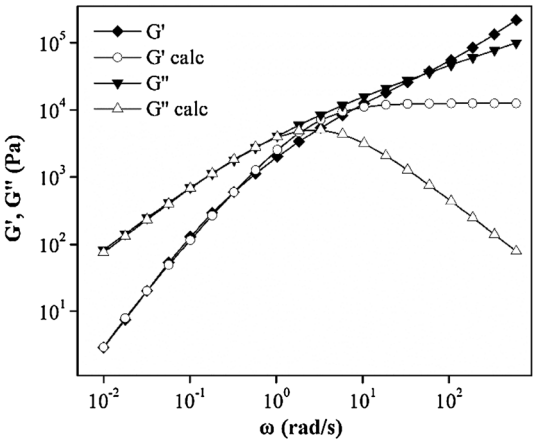

Fig. 4 G' and G'' of EVA along with their calculated values using the generalized Maxwell model

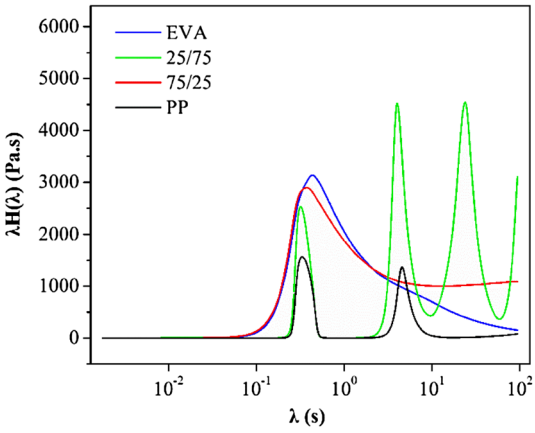

Fig. 5 Weighted relaxation spectra of PP, EVA, and PP/EVA blends

bulk relaxation of polymer melt could be a sign of presence of one and two molecular weight distributions [25] in EVA and PP, respectively. In addition, the smaller height of relaxation peaks of PP in comparison with that of EVA is due to lower viscosity of PP. The 75/25 PP/EVA blend shows one relaxation peak similar to that of EVA which its tail has been extended to higher relaxations times, without any further relaxation peak. In addition the relaxation peaks of matrix (PP) are unobservable, apparently. It seems that because of greater height of EVA relaxation peak, the first relaxation peak of PP has been overlapped by the EVA relaxation peak and presence of extended straight line prevents appearance of the second relaxation peak of PP. The extended line also indicates that shape relaxation of disperse phase in this blend takes place at considerably longer times. This is due to the higher viscosity of dispersed EVA particles and/or stronger interfacial adhesion between phases (as mentioned before in interpretation of the G' results). It can be expect that by increasing temperature during rheological measurements, the

deformed high viscous EVA particles may retract more easily, and consequently, the shape relaxation peak can appear at shorter times. Unlike the 75/25 blend, in the case of 25/75 blend, three separate relaxation peaks along with a tendency to upwards at high relaxation times are seen. The first two peaks relate to the bulk relaxation of PP and EVA and the third one and its tendency to get upwards at higher relaxation times can be attributed to the shape relaxation of dispersed PP domains within the EVA matrix. In our previous study on miscibility of PP/EVA blends, it was indicated that miscibility of PP/EVA blends is mainly due to the penetration of EVA chains within the PP molecules [8]. Therefore, the increase in height of PP relaxation peaks can be attributed to miscibility of high viscous EVA chains with PP. Moreover, the presence of two relaxation processes for interface (a single peak and a tail at the end of curve) can be attributed to the size inhomogeneity of dispersed phase.

Effect of LDH loading on relaxation spectrum of PP and EVA has been demonstrated in Fig. 6a, b, respectively. The first point to note is the considerable higher height of curves at longer relaxation times for EVA/LDH systems in comparison with PP/EVA hybrids which as mentioned before it stems from higher tendency of LDH to EVA. By increasing LDH loading, generally in both series of samples, their relaxation times increase considerably. In addition, when 1 and 3 wt. % of LDH have been added into EVA and PP, respectively, the trend of relaxation curves changes. This indicates that the presence of LDH at these weight percentages changes the relaxation modes of polymer chains. Appearance of new relaxation modes can be attributed to a change in molecular structure of polymer chains, for example, it has been reported that degradation of polymer chains may take place in presence of nanofiller during melt compounding [26].

Figure 7 indicates the effect of LDH loading on PP/EVA counterpart blends. Again, the greater height of relaxation curves at longer relaxation times for the EVA-rich hybrids is clearly evident. Also by addition of LDH into neat 75/25 blend, two significant changes in its relaxation curve occur: (1) straight tail in 75/25 blend is replaced by two relaxation peaks (one complete relaxation peak and an upward tendency at the end of the curve) and (2) both of the relaxation peaks of PP reappear.

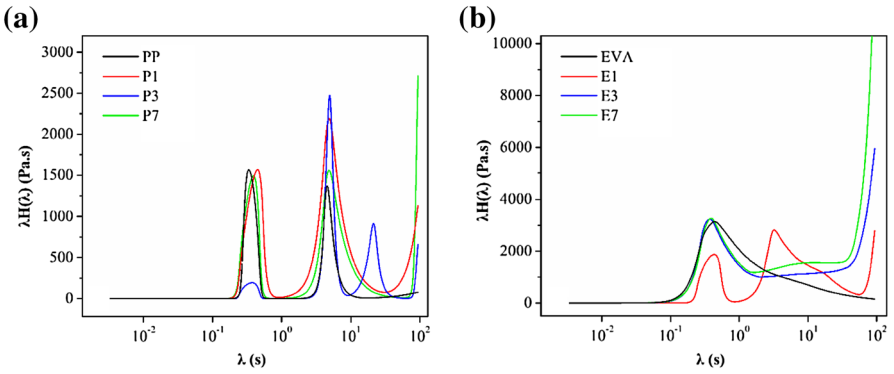

Fig. 6 Weighted relaxation spectrum of **a** PP/LDH and **b** EVA/LDH hybrids

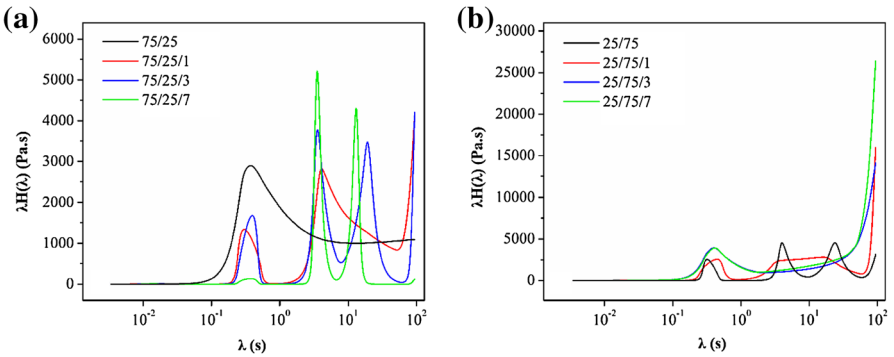

Fig. 7 Weighted relaxation spectrum of **a** 75/25/LDH and **b** 25/75/LDH hybrids

This observation is in line with the previously predicted results on localization of LDH platelets at the interface and mainly in EVA droplets in 75/25/LDH series of samples. In these samples, LDH platelets localized at the interface act as compatibilizer and, hence, affect the relaxation of interface, and result in appearance of interfacial relaxation at shorter times. In addition, since at these loadings of LDH, all the droplets have not interaction with LDH at their interface, there should be a kind of size inhomogeneity which appears as the two interfacial relaxation modes. Also that parts of LDH platelets which have been localized within the EVA droplets restrict the mobility of EVA chains and increase their relaxation time; therefore, EVA chains at these samples, unlike the neat blend, do not interact with PP chains or penetrate within that phase, and consequently, the characteristics relaxation peaks of PP appear in a more apparent manner. On the other hand, it seems that localization of main part of LDH at the matrix of 25/75/LDH hybrids as a result of enhancement of matrix viscosity could produce uniform morphology of dispersed phase during compounding which consequently at high LDH content, it leads to the disappearance of second interfacial relaxation peak.

According to the Maxwell model at the terminal region, G' and G'' are proportional to ω^2 and ω, respectively. For the neat polymers, these relations are satisfied completely. In the filled systems by increasing concentration of filler, an upward tendency in G' and G'' curves (especially in G') at low frequencies is seen. At higher filler concentrations, when the filler network is formed, a complete independency of G' from frequency is observed and G' curve lies above G'' values. The appearance of plateau in lower frequency ranges of G' curve for the intermediate filler loadings is along with appearance of second crossover in low-frequency ranges and completely staying above G'' curve for the higher concentrations of filler, known as solid-like behavior [27]. By calculation of G' and G'' exponents against ω, for different samples and tabulating the results in Table 1, it is seen that generally LDH incorporation results in reduction of both exponents. However, in none of the samples, complete independency of G' from frequency is not observable. Also for all the samples, only one crossover point between G' and G'' curves was detected that those values generally have descending

trend against LDH loading. The absence of complete solid-like behavior and second crossover point even at 7 wt% of LDH loading imply that the creation of solid networks of LDH platelets is impossible. The absence of solid-like behavior at 7 wt% of LDH could have two reasons: (1) this concentration of LDH is very low, and if even all the LDH platelets are exfoliated and distributed uniformly as single layers within the polymeric media, they will not create network-like structures, or (2) although the concentration of LDH is enough for creation of filler network, however, the filler particles have been not exfoliated to the extent that can create network-like structures. In addition, for the montmorillonite-filled systems, it has been observed that for the concentrations above 3–5 wt% of clay loading, where morphology of clay is a combination of exfoliated and intercalated structures, the second crossover point is observed. Since LDH has almost similar structure and density as of montmorillonite, it seems that the absence of solid-like behavior in the case of LDH-filled samples results mainly from the second hypostasis, i.e., lack of exfoliated and intercalated LDH layers and not as a result of low concentration of filler.

Morphology

TEM micrographs of 75/25/3 and 25/75/3 samples have been represented in Fig. 8. It is seen that in PP-rich sample as it was predicted, the LDH platelets have been localized only at the interface and in the EVA droplets. In addition, the LDH particles have been not intercalated or exfoliated. On the other hand, in the case of EVA-rich hybrid, the LDH particles have mainly been situated within the matrix phase. In addition, extend of intercalated structures in this blend is slightly more

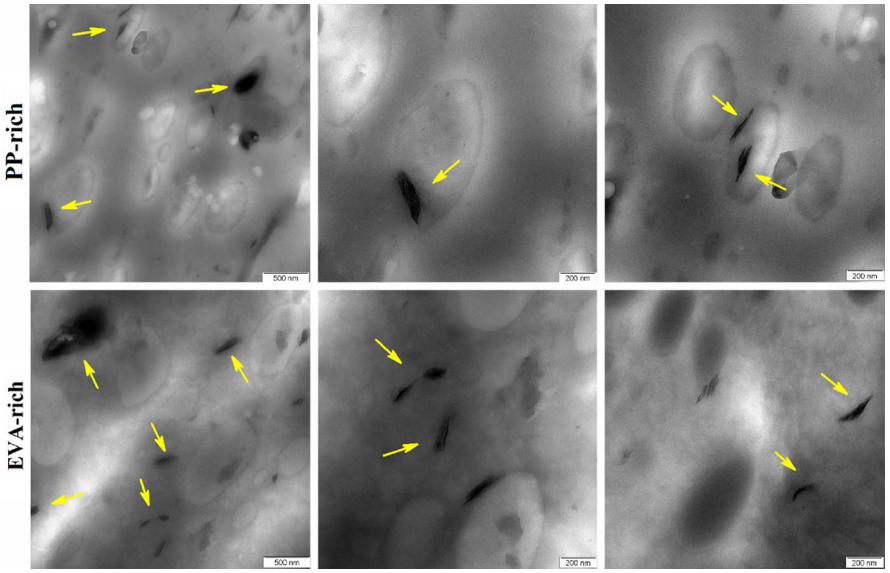

Fig. 8 TEM micrographs of 75/25/3 (*upper three images*) and 25/75/3 (*lower three images*)

than that of the counterpart system. However, it should be noted that in both of these systems, as it was predicted the extent of exfoliated and intercalated structures is considerably low. In general, it can be concluded from this observation that to obtain polymeric nanocomposites based on LDH, solely using melt mixing method is not enough and it is better to use specific methods to intercalate and exfoliate LDH layers. The strategies, such as implementation of effective compatibilizer or other preparation methods like solvent or polymerization techniques can be helpful.

Conclusion

Counterpart blends of PP and EVA along with their pure components and their corresponding organo-modified LDH loaded composites were prepared in a one-step melt compounding process in a twin-screw micro compounder. SAOS experiment was conducted to study the rheological properties of the developed systems. It was found that presence of LDH increases the storage modulus and complex viscosity, especially in the terminal region. However, this increment was not as high as the situation, in which the filler network was formed. In addition, the elasticity enhancement in EVA-rich hybrids was higher as compared to the enhancement observed in the counterpart PP-rich hybrids. This observation was attributed to the grater affinity of LDH to EVA rather than to PP. Moreover, by comparing the elasticity values between PP-rich/LDH and EVA-rich/LDH hybrids, it was predicted that LDH platelets in the case of PP-rich samples have been located at interface or within the EVA dispersed particles, while in the case of EVA-rich samples, they mainly localized within the matrix. In continue, to investigate the recorded data in a more quantitative manner, two approaches were used: (1) GNF and (2) GLVE model approaches. In the former approach using Carreau–Yasuda viscosity model and also Cox-Merz rule, all the model parameters for complex viscosity curves were calculated, and the alteration in the calculated parameters as a function of LDH loading was correlated to the physical effects of LDH. However, the observed trend for the relaxation time calculated based on Carreau–Yasuda model was not meaningful. The physically meaningless values of calculated relaxation time from the Carreau–Yasuda model was interpreted in terms of drawback of the GNF approach in considering memory effects in the calculation of relaxation times. Therefore, the GLVE approach was used to obtain reliable and interpretable relaxation times. Relaxation time spectrum of samples was calculated using fitting of generalized Maxwell model into the experimental data of G' and G''. Alteration in relaxation spectrum of samples was interpreted in terms of change in homogeneity of blend and in the case of LDH-loaded samples in terms of imposed restriction against chain mobility and its partitioning between phases in ternary hybrids. In addition, the crossover frequency and slope of G' and G'' curve at terminal region were calculated and correlated with the extent of intercalated and exfoliated structures of filler. Finally, using TEM micrographs, the filler morphology and LDH platelets localization was investigated, and it was found that the results were well consistent with the predictions made based on rheological data.

References

1. Lu Y, An L, Wang S-Q, Wang Z-G (2015) Molecular mechanisms for conformational and rheological responses of entangled polymer melts to startup shear. Macromolecules 48(12):4164–4173
2. Hoyle D, Auhl D, Harlen O, Barroso V, Wilhelm M, McLeish T (2014) Large amplitude oscillatory shear and Fourier transform rheology analysis of branched polymer melts. J Rheol (1978-present) 58(4):969–997
3. D'Avino G, Greco F, Hulsen M, Maffettone PL (2013) Rheology of viscoelastic suspensions of spheres under small and large amplitude oscillatory shear by numerical simulations. J Rheol (1978-present) 57(3):813–839
4. Morrison FA (2001) Understanding rheology. Oxford University Press, USA
5. Aghjeh MR, Nazari M, Khonakdar HA, Jafari SH, Wagenknecht U, Heinrich G (2015) In depth analysis of micro-mechanism of mechanical property alternations in PLA/EVA/clay nanocomposites: a combined theoretical and experimental approach. Mater Design 88:1277–1289
6. Da Silva ALN, Rocha MC, Coutinho F, Bretas RE, Scuracchio C (2001) Rheological and thermal properties of binary blends of polypropylene and poly (ethylene-CO-1-octene). J Appl Polym Sci 79(9):1634–1639
7. Aghjeh MR, Khonakdar HA, Jafari SH, Zschech C, Gohs U, Heinrich G (2016) Rheological, morphological and mechanical investigations on ethylene octene copolymer toughened polypropylene prepared by continuous electron induced reactive processing. RSC Advances
8. Aghjeh MR, Khonakdar HA, Jafari SH (2015) Application of mean-field theory in PP/EVA blends by focusing on dynamic mechanical properties in correlation with miscibility analysis. Compos Part B Eng 79:74–82
9. Valera-Zaragoza M, Ramírez-Vargas E, Medellin-Rodriguez F, Huerta-Martinez B (2006) Thermal stability and flammability properties of heterophasic PP–EP/EVA/organoclay nanocomposites. Polym Degrad Stab 91(6):1319–1325
10. Lonkar SP, Therias S, Leroux F, Gardette JL, Singh RP (2011) Influence of reactive compatibilization on the structure and properties of PP/LDH nanocomposites. Polym Int 60(12):1688–1696
11. Du L, Qu B, Meng Y, Zhu Q (2006) Structural characterization and thermal and mechanical properties of poly (propylene carbonate)/MgAl-LDH exfoliation nanocomposite via solution intercalation. Compos Sci Technol 66(7):913–918
12. Aghjeh MR, Asadi V, Mehdijabbar P, Khonakdar HA, Jafari SH (2016) Application of linear rheology in determination of nanoclay localization in PLA/EVA/Clay nanocomposites: correlation with microstructure and thermal properties. Compos Part B Eng 86:273–284
13. Sharma V, Jaishankar A, Wang Y-C, McKinley GH (2011) Rheology of globular proteins: apparent yield stress, high shear rate viscosity and interfacial viscoelasticity of bovine serum albumin solutions. Soft Matter 7(11):5150–5160
14. Qiao J, Guo M, Wang L, Liu D, Zhang X, Yu L, Song W, Liu Y (2011) Recent advances in polyolefin technology. Polym Chem 2(8):1611–1623
15. Faker M, Aghjeh MR, Ghaffari M, Seyyedi S (2008) Rheology, morphology and mechanical properties of polyethylene/ethylene vinyl acetate copolymer (PE/EVA) blends. Eur Polym J 44(6):1834–1842
16. Sun G, Li H (2006) Influence of intercalated montmorillonite/polyethylene glycol binary processing aids on the rheological and mechanical properties of metallocene linear low-density polyethylene. Polym Bull 57(6):963–973
17. Goodarzi V, Jafari SH, Khonakdar HA, Seyfi J (2011) Morphology, rheology and dynamic mechanical properties of PP/EVA/clay nanocomposites. J Polym Res 18(6):1829–1839
18. Wu D, Zhang Y, Zhang M, Yu W (2009) Selective localization of multiwalled carbon nanotubes in poly (ε-caprolactone)/polylactide blend. Biomacromolecules 10(2):417–424
19. Bird RB, Armstrong RC, Hassager O, Curtiss CF (1977) Dynamics of polymeric liquids, vol 1. Wiley, New York
20. Sousa PC, Pinho FT, Oliveira MS, Alves MA (2012) High performance microfluidic rectifiers for viscoelastic fluid flow. RSC Adv 2(3):920–929
21. Bird RB, Armstrong R, Hassager O (1987) Dynamics of polymeric liquids. Vol. 1: Fluid mechanics
22. Orbey N, Dealy JM (1991) Determination of the relaxation spectrum from oscillatory shear data. J Rheol (1978-present) 35(6):1035–1049

23. Basseri G, Mazidi MM, Hosseini F, Aghjeh MR (2014) Relationship among microstructure, linear viscoelastic behavior and mechanical properties of SBS triblock copolymer-compatibilized PP/SAN blend. Polym Bull 71(2):465–486
24. Roths T, Maier D, Friedrich C, Marth M, Honerkamp J (2000) Determination of the relaxation time spectrum from dynamic moduli using an edge preserving regularization method. Rheol Acta 39(2):163–173
25. Shahbazi K, Aghjeh MR, Abbasi F, Meran MP, Mazidi MM (2012) Rheology, morphology and tensile properties of reactive compatibilized polyethylene/polystyrene blends via Friedel-Crafts alkylation reaction. Polym Bull 69(2):241–259
26. Xu X, Ding Y, Qian Z, Wang F, Wen B, Zhou H, Zhang S, Yang M (2009) Degradation of poly (ethylene terephthalate)/clay nanocomposites during melt extrusion: effect of clay catalysis and chain extension. Polym Degrad Stab 94(1):113–123
27. Mizuno C, John B, Okamoto M (2013) Percolated network structure formation and rheological properties in nylon 6/clay nanocomposites. Macromol Mater Eng 298(4):400–411